obtained diffusivity of the order of 10^{-14} m^2 s^{-1} is in satisfactory agreement with the results of previous uptake experiments.

Acknowledgment. Stimulating discussions with C. Dybowski, in particular about refs 20 and 21, are gratefully acknowledged. Both the group in Leipzig and the group in Stuttgart express their gratitude to the German Science Foundation (Deutsche Forschungsgemeinschaft) for financial support.

Registry No. ^{129}Xe, 13965-99-6; C_6H_6, 71-43-2.

References and Notes

(1) Ruthven, D. M. *Principles of Adsorption and Adsorption Processes*; Wiley: New York, 1984.
(2) Kärger, J.; Ruthven, D. M. *Zeolites* **1989**, *9*, 267.
(3) Stejskal, E. O.; Tanner, J. E. *J. Chem. Phys.* **1965**, *42*, 288.
(4) Kärger, J.; Heink, W. *J. Magn. Reson.* **1983**, *51*, 1.
(5) Kärger, J.; Pfeifer, H.; Rudtsch, S. *J. Magn. Reson.* **1989**, *85*, 381.
(6) Cohen de Lara, E.; Kahn, R.; Mezei, F. *J. Chem. Soc., Faraday Trans. 1* **1983**, *79*, 1911.
(7) Jobic, H.; Bée, M.; Caro, J.; Kärger, J.; Bülow, M. *J. Chem. Soc., Faraday Trans. 1* **1989**, *85*, 4201.
(8) June, R. L.; Bell, A. T.; Theodorou, D. N. *J. Phys. Chem.* **1990**, *94*, 8232.
(9) Pickett, S. D.; Nowak, A. K.; Thomas, J. M.; Peterson, L. K.; Swift, J. F. P.; Cheetham, A. K.; den Ouden, C. J. J.; Smit, B.; Post, M. F. M. *J. Phys. Chem.* **1990**, *94*, 4329.
(10) Goodbody, S. J.; Watanabe, K.; MacGowan, D.; Walton, J. P. R. B.; Quirke, N. *J. Chem. Soc., Faraday Trans.* **1991**, *87*, 1951.
(11) Barrer, R. M. *Zeolites and Clay Minerals as Adsorbents and Catalysts*; Academic Press: London, 1978.
(12) Hayhurst, D. T.; Paravar, A. R. *Zeolites* **1988**, *8*, 27.
(13) Van den Begin, N. G.; Rees, L. V. C.; Caro, J.; Bülow, M. *Zeolites* **1989**, *9*, 287.
(14) Jameson, A. K.; Jameson, C. J.; Gutowski, H. S. *J. Chem. Phys.* **1973**, *59*, 4540.
(15) Ito, T.; Fraissard, J. In *Proceedings of the 5th International Conference on Zeolites, Naples, 1980*; Rees, L. V. C., Ed.; Heyden: London, 1980; p 510.
(16) Fraissard, J.; Ito, T. *Zeolites* **1989**, *8*, 350.
(17) Ripmeester, J. *J. Am. Chem. Soc.* **1982**, *104*, 289.
(18) Gedeon, A.; Ito, T.; Fraissard, J. *Zeolites* **1988**, *8*, 376.
(19) Chmelka, B. F.; Gillis, J. V.; Petersen, E. E.; Radke, C. J. *AIChE J.* **1990**, *36*, 1562.
(20) Bansal, N.; Dybowski, C. *J. Magn. Reson.* **1990**, *89*, 21.
(21) Kärger, J. *J. Magn. Reson.* **1991**, *93*, 184.
(22) Struve, P.; Kočiřík, M.; Bülow, M.; Zikánová, A.; Bezus, A. G. *Z. Phys. Chem. (Leipzig)* **1983**, *264*, 49.
(23) Doelle, H. J.; Riekert, L. *ACS Symp. Ser.* **1977**, *40*, 401.
(24) Chihara, K.; Suzuki, M.; Kawazoe, K. *Chem. Eng. Sci.* **1976**, *31*, 505.
(25) Ruthven, D. M.; Lee, L.-K. *AIChE J.* **1981**, *27*, 654.
(26) Karge, H. G.; Niessen, W. *Catal. Today* **1991**, *8*, 451.
(27) Crank, J. *The Mathematics of Diffusion*; Clarendon Press: Oxford, 1956.
(28) Kärger, J. *AIChE J.* **1982**, *28*, 417.
(29) Müller, U.; Unger, K. K. *Zeolites* **1988**, *8*, 154.
(30) Heink, W.; Kärger, J.; Pfeifer, H.; Stallmach, F. *J. Am. Chem. Soc.* **1990**, *112*, 2175.
(31) Förste, C.; Germanus, A.; Kärger, J.; Pfeifer, H.; Caro, J.; Pilz, W.; Zikánová, A. *J. Chem. Soc., Faraday Trans. 1* **1987**, *83*, 2301.
(32) Zikánová, A.; Bülow, M.; Schlodder, H. *Zeolites* **1987**, *7*, 115.
(33) Beschmann, K.; Kokotailo, G. T.; Riekert, L. *Chem. Eng. Process.* **1987**, *22*, 223.
(34) Shah, D. B.; Hayhurst, D. T.; Evanina, G.; Guo, C. J. *AIChE J.* **1988**, *34*, 1713.
(35) Förste, C.; Kärger, J.; Pfeifer, H.; Riekert, L.; Bülow, M.; Zikánová, A. *J. Chem. Soc., Faraday Trans. 1* **1990**, *86*, 881.
(36) Kärger, J.; Zikánová, A.; Kočiřík, M. *Z. Phys. Chem. (Leipzig)* **1984**, *265*, 587.
(37) Hong, U.; Kärger, J.; Pfeifer, H. *J. Am. Chem. Soc.* **1991**, *113*, 4812.

Competition between C–O and 1-C–H Bond Scission during Deoxygenation: The Reactions of 1-Propanol on Mo(110)

Benjamin C. Wiegand, P. Uvdal, J. G. Serafin, and C. M. Friend*

Department of Chemistry, Harvard University, Cambridge, Massachusetts 02138 *(Received: January 2, 1992; In Final Form: February 25, 1992)*

The reactions of 1-propanol on Mo(110) were investigated using temperature programmed reaction and high resolution electron energy loss and X-ray photoelectron spectroscopies. 1-Propanol forms 1-propoxide upon adsorption on Mo(110) at 120 K. An intensity analysis of the vibrational data indicates that the C–O bond vector is nearly perpendicular to the surface. Vibrational data also suggest that the C–O bond is weakened in 1-propoxide relative to 1-propanol. The 1-propoxide intermediate is stable up to 375 K, at which point it decomposes via three competing pathways: deoxygenation and dehydrogenation to form propene, the major hydrocarbon product; C–O bond hydrogenolysis to afford propane; and nonselective decomposition to gaseous dihydrogen, surface carbon, and surface oxygen. The reaction of isotopically-labeled 1-propanol shows that only the C–H bond at the 2 position (γ to the metal and β to the oxygen) in 1-propoxide is broken during propene formation. Carbon–oxygen bond scission is proposed to limit the rate of propene elimination. Conversely, dehydrogenation at the 1-carbon of 1-propoxide is proposed to limit the rate of nonselective decomposition. At the maximum coverage of 1-propoxide, ~60% of the adsorbed 1-propoxide forms hydrocarbons, whereas ~40% nonselectively decomposes. The reactions of 1-propanol are compared with 2-propanol and 1-propanethiol in an effort to delineate the controlling factors in deoxygenation kinetics.

Introduction

The reactions of oxygen-containing molecules are of great importance due to their presence in feedstocks and in adhesive materials. They also serve as models for the microscopic reverse of Fisher–Tropsch synthesis. The reactions of primary and secondary alcohols have been previously observed to have widely different reaction kinetics. On Fe(100), primary alcohols formed a stable alkoxide.[1] In the reaction of ethanol, ethoxide underwent competing C–C and C–O bond scission along with nonselective decomposition. On the other hand, added steric interactions of the second methyl group in 2-propanol were proposed to account for the fact that 2-propoxide is not formed on Fe(100); acetone was the major product.[1] On Pd(111), both primary and secondary alcohols formed surface alkoxides which underwent 1-C–H bond scission forming an acyl intermediate.[2,3] The C–C bond adjacent to the oxygen is cleaved in the acyl intermediate yielding ethylene and CO from 1-propanol. However, acetone, methane, and CO were the major products formed from 2-propanol reaction on Pd(111). Slower kinetics for C–C bond scission in the acetone intermediate were proposed to account for the different product distributions.[2,3]

Previously, the reaction of 2-propanol was investigated on Mo(110).[4] The O–H bond in 2-propanol is cleaved upon adsorption to form a 2-propoxide intermediate. 2-Propoxide is stable up to ~350 K, where it undergoes C–O and 2-C–H bond scission to form propene as the major product. C–O bond hydrogenolysis to form propane is also a minor pathway. Nonselective decomposition to atomic carbon, oxygen, and gaseous dihydrogen is also a competing process. There was only a minor kinetic isotope effect in the reactions of various selectively deuterated 2-propanol iso-

0022-3654/92/2096-5063$03.00/0

topomers to eliminate propene. Thus, the rate-limiting step was proposed to be C–O bond cleavage. This result was in direct contrast to reactions of alcohols on mid- and late-transition metals, such as Cu(110) and Ag(110), where the kinetic stabilities of alkoxides have been correlated with the strength of the C–H bond on the carbon bound directly to oxygen.[5-7] Importantly, on late-transition metals, C–O bond retention in alcohols is seen for all cases except for the reaction of methanol on Pt(110).[8]

In an effort to learn more about the controlling factors in alkoxide deoxygenation on Mo(110), the reaction of 1-propanol was studied on Mo(110). In this study, carbon–oxygen bond scission in 1-propanol is compared to 2-propanol in order to discern the effect of alkyl substitution on deoxygenation kinetics and selectivity.

Experimental Section

Experiments were performed in two different ultrahigh vacuum chambers with base pressures of 1.5×10^{-10} Torr. Both have been described in detail previously.[4,9] One chamber was used for X-ray photoelectron and temperature programmed reaction experiments, while the other was used solely for high resolution electron energy loss experiments. The Mo(110) single crystal was prepared as described previously.[10] A heating rate of 15 ± 1 K/s was used in all temperature programmed reaction experiments unless otherwise noted.

The electron energy loss spectrometer was operated at a primary electron energy of 3 eV and had a spectral resolution of 50–80 cm^{-1} [6.5–10 meV]. The resolution varied because of the distinctly different surface reflectivities for monolayer and multilayer coverages. The spectra were collected both off- and on-specular directions as noted in the text. Fourier transform infrared spectra of the gas-phase 1-propanol isotopomers were collected on a Nicolet 800 system.

Mass spectrometry was used to identify the products formed during temperature programmed reaction. Propene was identified as the product of 1-propanol reaction based on the m/e 41:m/e 42 ratio of 1.6:1.0, which is identical to that measured for an authentic sample of propene in our mass spectrometer within experimental error. The fragmentation patterns of propene-d_2 and propene-d_3 were also determined in order to clearly identify the products derived from the isotopically-labeled 1-propanols. For propene-d_2, the relative ratios of m/e 42, 43, 44, and 45 were measured to be 0.42:1.00:0.78:0.03, while for propene-d_3, the relative intensities of m/e 43, 44, and 45 were 0.69:1.04:1.00.

1-Propanol was obtained from Fischer with 99+% purity and used without further purification. 1-Propanol-1,1-d_2 (99% D), 1-propanol-2,2-d_2 (98.5% D), and 1-propanol-3,3,3-d_3 (99% D) were purchased from MSD Isotopes and used as received. The alcohols were purified by successive freeze–pump–thaw cycles before use each day, and their purity was confirmed by mass spectrometry. Propene-d_2 (99.7% D) was purchased from MSD Isotopes, and propene-d_3 (99% D) was purchased from Cambridge Isotope Laboratories; both were used as received. Directed dosing of the crystal at a crystal temperature of 120 K was used in all cases so that the chamber pressure remained below 3×10^{-10} Torr during dosing. Oxygen (Matheson, Extra Dry, 99.6%) was used to clean the crystal after temperature programmed reaction.

Results

I. Temperature Programmed Reaction of 1-Propanol on Mo(110) at Saturation Exposure. Propene is the primary hydrocarbon product during reaction of 1-propanol on Mo(110) (Figure 1). A minor amount of propane is also produced. Nonselective decomposition to adsorbed carbon, oxygen, and gaseous dihydrogen is the third competing pathway. All masses between m/e 2 and 80 were monitored during the reaction of 1-propanol; propene, propane, and H_2 were the only detectable gas–phase reaction products. Condensed layers of 1-propanol sublime at ~185 K, evident as the sharp peak in the m/e 31 spectrum (Figure 1). There is a tail on the 1-propanol peak that extends to ~400 K but no desorption above 400 K. No other oxygen-containing or hydrocarbon products were detected.

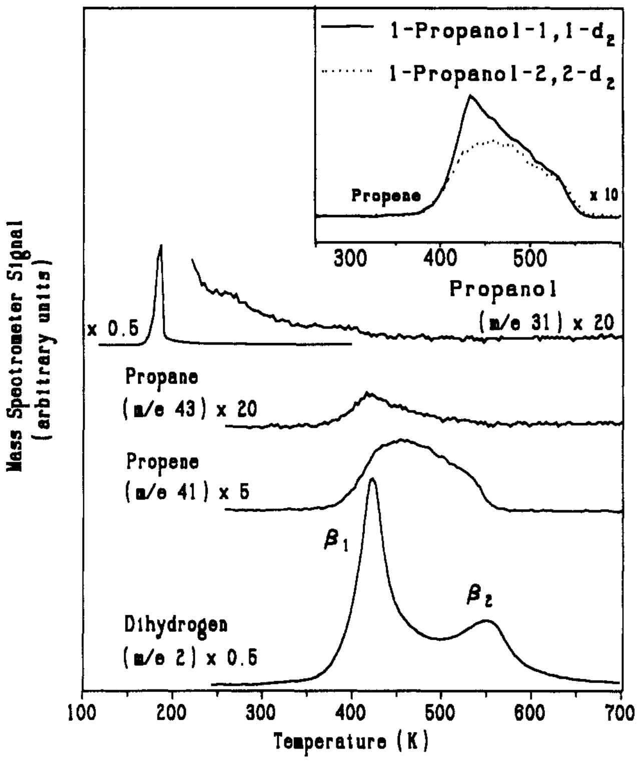

Figure 1. Temperature programmed reaction data obtained during reaction of 1-propanol at saturation exposure on Mo(110). Multiplication factors refer to the uncorrected relative intensity of the masses shown. Propene and propane formation from temperature programmed reaction of 1-propanol-1,1-d_2 (solid lines) and 1-propanol-2,2-d_2 (dotted lines) are shown in the inset. The parent ions are shown for all products formed: m/e 43, propene-d_1; m/e 44, propene-d_2; and m/e 46, propane-d_2. None of the data are corrected for fragmentation. The fragmentation of propane to 41 amu accounts for ~1% of the intensity.

Propene formation commences at ~375 K and continues until ~560 K. The product is identified as propene, not cyclopropane, based on the m/e 41:m/e 42 ratio of 1.6. Propane formation also commences at ~375 K, reaching a maximum at 425 K and continuing to evolve in a tail reaching up to ~525 K. The amount of propene formed relative to propane is estimated to be ~6:1,[11] compared to ~20:1 for the reaction of 2-propanol on Mo(110).

The rate of gaseous propene evolution at 420 K is limited by the rate of reaction, not by the desorption of propene. Propene desorbs at temperatures below 300 K, both when adsorbed on initially clean Mo(110) or when coadsorbed with alcohols on Mo(110) (data not shown).[4] In contrast, propene is evolved *above* 300 K during 1-propoxide decomposition.

Dihydrogen formation commences at ~350 K and goes through two maxima at 425 K (β_1) and 555 K (β_2) (Figure 1). The ratio of the β_1:β_2 areas is ~1.6:1 for the reaction of 1-propanol on Mo(110). The maximum of the β_1 dihydrogen peak is essentially identical to the maximum of the propane peak.

No deuterium is incorporated into the propene formed during temperature programmed reaction of a mixture of 1-propanol and deuterium on Mo(110); only propene-d_0 is detected. The lack of deuterium incorporation into the propene product demonstrates that no reversible C–H bond activation occurs during propene formation and is consistent with a unimolecular decomposition to form propene. Only one deuterium was incorporated into the propane formed; no propane-d_2 or higher deuterated propanes were detected.

One of the 2-C–H bonds is selectively cleaved during the elimination of propene from 1-propanol on Mo(110) based on temperature programmed reaction of 1-propanol-1,1-d_2, -2,2-d_2, and -3,3,3-d_3. Propene-d_1 is the sole propene product formed during temperature programmed reaction of 1-propanol-2,2-d_2 (data not shown). There is a minor m/e 44 signal from the reaction of 1-propanol-2,2-d_2 on Mo(110); however, this intensity is due entirely to contributions from the propane-d_2 and propene-d_1

TABLE I: Integration of β_1 and β_2 Dihydrogen Peaks in the 1-Propanol Isotopomers[36]

	β_1:β_2 peak ratios		
molecule	H_2	HD	D_2
1-propanol-1,1-d_2	2.1	1.7	1.2
1-propanol-2,2-d_2	1.8	1.4	1.0
1-propanol-3,3,3-d_3	2.3	1.1	0.4
1-propanol	1.6		

formed.[12] Similarly, propene-d_2 is formed during temperature programmed reaction of 1-propanol-1,1-d_2: No propene-d_1 is detected based on comparison of the fragmentation patterns for the product and that previously measured for a propene-d_2 sample. Likewise, the reaction of 1-propanol-3,3,3-d_3 exclusively produced propene-d_3, indicating that no methyl C–H bonds are broken during propene formation.

There is a relatively small kinetic isotope effect for the kinetics and yields of propene for 1-propanol-1,1-d_2, but none measurable for the other isotopically-labeled 1-propanols.[13] Temperature programmed reaction of the isotopically labeled 1-propanols showed that for 1-propanol-1,1-d_2, the kinetics and relative amount of propene formation were increased relative to 1-propanol-2,2-d_2 (Figure 1 inset). The kinetics for propene formation during the reaction of 1-propanol-2,2-d_2 on Mo(110) are identical to 1-propanol-3,3,3-d_3 and 1-propanol-d_0 within experimental error (data not shown). There are also no major differences in the propane formation kinetics for the other three isotopes.

The selective labeling experiments also demonstrate that 1-C–H bond scission commences near 350 K. Since 1-C–H(D) breaking does *not* afford propene, any β_1 dideuterium produced from 1-propanol-1,1-d_2 must be from nonselective decomposition. All dihydrogen isotopes are evolved more slowly from 1-propanol-1,1-d_2 than from 1-propanol-2,2-d_2. These data suggest that dehydrogenation at the 1-position is more rapid than at the 2-position.

The isotopic distributions for β_1 and β_2 dihydrogen suggest that 1-C–H bond scission is more facile than 2-C–H bond cleavage in 1-propanol adsorbed on Mo(110). Furthermore, 3-C–H bond breaking is shown to be the least rapid. The relative amounts of the β_1 and β_2 peaks for H_2, HD, and D_2 for the three different selectively-labeled 1-propanols indicate the relative kinetics for 1, 2, and 3 dehydrogenation (Table I). The β_1 dihydrogen peak contains contributions from the alcoholic proton, nonselective C–H bond scission, and selective 2-C–H bond breaking to yield propene. The β_2 peak arises completely from nonselective dehydrogenation.

Carbon–hydrogen bond breaking in the methyl group is the slowest and primarily occurs above 475 K as is demonstrated by the ratio of β_1- to β_2-D_2 of 0.4 in the reaction of 1-propanol-3,3,3-d_3 (Table I). The β_1-D_2:β_2-D_2 ratio is highest for 1-propanol-1,1-d_2, indicating that 1-dehydrogenation is most facile. Selective deuteration at the 2-position yields an intermediate value for the ratio, indicating that it occurs at an intermediate rate. The β_1:β_2 ratios cannot be analyzed in more detail since they envelope a convolution of competing processes.

II. X-ray Photoelectron Spectroscopy. X-ray photoelectron data are stong evidence that 1-propoxide is the major surface species up to the onset of hydrocarbon formation on Mo(110) (Figure 2). These data are consistent with formation of 1-propoxide at 200 K, above the multilayer sublimation temperature, and its persistence up to the onset of propene formation.

X-ray photoelectron spectra of 1-propanol multilayers were obtained as reference data (Figure 2a(i)). The C(1s) spectrum for 1-propanol multilayers was fit with two peaks at 287.7 and 286.3 eV in a ratio of 1:2. These peaks are respectively assigned to the carbon bound to oxygen and to the other two carbons in 1-propanol. The 1.4 eV energy difference between the peaks is consistent with that expected for molecules containing C–O bonds.[14] The values are also in good agreement with those measured for 2-propanol on Mo(110).[4]

One major O(1s) peak with a binding energy of 534.1 eV is observed for 1-propanol multilayers (Figure 2b(i)), and is in agreement with those measured for 2-propanol multilayers. The small peak at 532.2 eV is ascribed to 1-propoxide in the first layer.

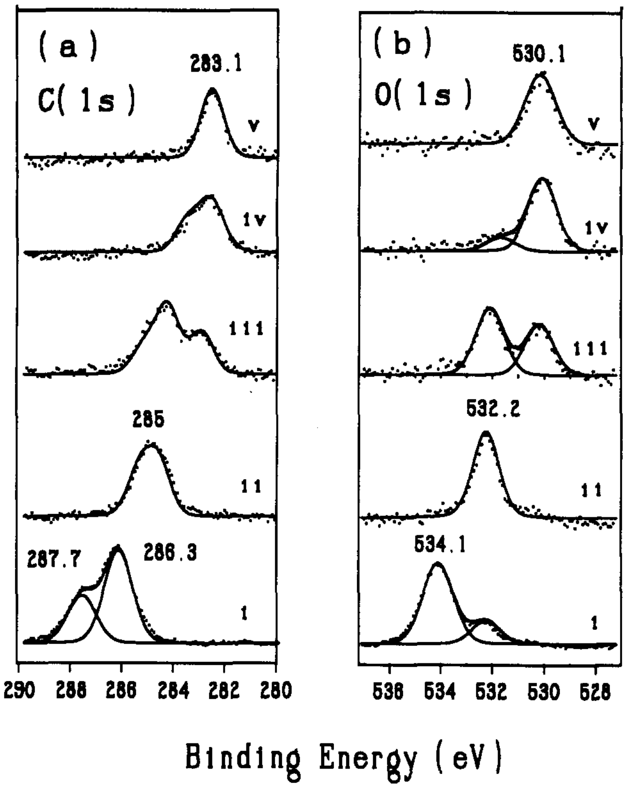

Figure 2. (a) O(1s) and (b) C(1s) X-ray photoelectron spectra obtained after adsorbing 1-propanol multilayers on Mo(110) at 120 K followed by (i) no annealing, (ii) annealing to 300 K, (iii) annealing to 400 K, (iv) annealing to 500 K, and (v) annealing to 750 K. The spectra were collected after the surface was cooled to 120 K.

X-ray photoelectron data unequivocally show that the majority of C–O bonds remain intact when 1-propanol is heated to 300 K and are consistent with cleavage of the O–H bond to generate 1-propoxide on the surface (Figure 2b(ii)). A single O(1s) peak at 532.2 eV is observed after annealing multilayers of 1-propanol to 300 K.

C(1s) X-ray photoelectron data are also consistent with the presence of a 1-propoxide intermediate at 300 K (Figure 2b(i)). Notably, there is little or no intensity near 283 eV, the binding energy expected for atomic carbon. The C(1s) peaks are not resolved when 1-propanol multilayers are annealed to 300 K; there is a broad peak with a full width at half-maximum of ~2 eV centered at ~285 eV, which is a convolution of more than one carbon environment. These data are similar to those obtained for 2-propoxide on Mo(110).[4] The splitting of the two peaks due to the inequivalent carbon environments in 1-propoxide may be smaller than for intact 1-propanol, which may account for the lack of resolution of two peaks. The broad peak may also envelope peaks due to hydrocarbon fragments, or an oxymetallacycle, which would have binding energies between 284 and 285 eV.[15]

Carbon–oxygen bond cleavage commences as 1-propoxide is heated above 350 K, the temperature required for propene formation. Upon heating, the O(1s) peak attributed to 1-propoxide attenuates and a peak at 530.1 eV, due to atomic oxygen, grows (Figure 2b(iii)). Only atomic oxygen is detected after heating 1-propanol multilayers to 500 K. A new C(1s) peak also appears at ~283 eV after heating to 400 K, indicating that some nonselective decomposition has occurred.

After annealing to 750 K, only atomic carbon and oxygen are present on the surface. One peak with a binding energy of 283.1 eV is detected in the C(1s) spectrum, which is ascribed entirely to atomic carbon. Similarly, the only oxygen-containing species left on the surface is atomic oxygen with a binding energy of 530.1 eV.

After reaction of 1-propanol to 750 K, the C:O peak area ratio, determined after correction for atomic sensitivity factors, is

TABLE II: Vibrational Assignments for 1-Propanol (in cm^{-1})

gas-phase 1-propanol		on Mo(110)			
		1-propanol multilayers		1-propoxide	
3667	ν(O–H)	3190	ν(O–H)		
2952	ν(C–H)	2930	ν(C–H)	2900	ν(C–H)
1462	$\delta_a(CH_3)$	1450	$\delta_a(CH_3)$	1440	$\delta_a(CH_3)$
1390	$\delta_s(CH_3)$	1380	$\delta_s(CH_3)$	1380	$\delta_s(CH_3)$
1226	δ(O–H)				
1064	ν(C–O)	1060	ν(C–O)	990	ν(C–O)
970	$\rho(CH_3)$				
893		890	ν_s(C–C)	890	ν_s(C–C)
		730	$\gamma(CH_2)$		
				580	ν(metal–OR)
		470	δ(CCO), δ(CCC)	380	δ(CCO), δ(CCC)

TABLE III: Vibrational Assignments for Isotopically-Labeled 1-Propoxide on Mo(110) (in cm^{-1})

	-d_0	-1,1-d_2	-2,2-d_2	-3,3,3-d_3
ν(C–H)	2900	2915	2940	2900
ν(C–D)		2125	2190	2200, 2090
$\delta_a(CH_3)$	1440	1460	1450	1440
$\delta_s(CH_3)$	1380	1372	1380	
$\delta_s(CD_3)$				1090
$\delta(CH_2)$				1350, 1440
$\delta(CD_2)$[37]		1080		
ν(C–O)	990	975	980	990
ν(C–C)	890		1195, 820	1090
ν(metal–OR)	580	580	590	590
δ(CCC), δ(CCO)	380	400	380	390

1.16:1.00. Since carbon leaves the surface only in the form of C_3-hydrocarbons and no gaseous oxygen-containing products are evolved, this ratio is a measure of the relative amount of nonselective decomposition to hydrocarbon formation. Accordingly, ~60% of the 1-propoxide forms hydrocarbons while the remaining ~40% nonselectively decomposes. The saturation coverage of 1-propoxide is determined to be 0.35 monolayer based on the O(1s) intensity relative to an ordered oxygen overlayer on Mo(110) with a coverage of 0.45 monolayer.[16,17]

III. High Resolution Electron Energy Loss Spectroscopy. High resolution electron energy loss data confirm that the major surface species up to the onset of hydrocarbon formation is 1-propoxide. The ν(O–H) mode disappears after annealing 1-propanol multilayers to 300 K, and there is a large increase in the intensity of the loss assigned as the ν(C–O) mode at ~980 cm^{-1}. Otherwise, only minor changes of the vibrational spectrum compared to 1-propanol multilayers are observed. The electron energy loss data shown in Figures 3 and 4 are summarized in Tables II and III along with gas-phase infrared assignments. Four different isotopomers of 1-propanol were studied, but spectra are only shown for 1-propanol-d_0 and -d_3. Spectra and gas-phase data for the other cases are available as supplementary material. Due to the inherent superior resolution in the infrared data, only the most intense features in the gas-phase data are included in Table II. All assignments are consistent with the observed shifts of the modes induced by isotopic labeling of the 1-propanols, which were essential in assigning the various losses in the electron energy loss spectra.

Reference spectra of condensed layers of 1-propanol have a prominent loss associated with the ν(O–H) mode at 3190 cm^{-1}, as well as losses characteristic of 1-propanol (Figures 3 and 4; Tables II and III). The frequency of the ν(O–H) mode agrees well with previous studies of 2-propanol on Mo(110) (3225 cm^{-1}).[4] As the methyl ν(C–H) modes are shifted down in the spectrum of 1-propanol-3,3,3-d_3 and the peak is more clearly resolved, the ν(O–H) mode is observed at 3230 cm^{-1} (Figure 4a). The lower O–H stretch frequency in 1-propanol multilayers compared to the gas phase is attributed to hydrogen bonding. The other losses are in good agreement with those calculated and observed for gas and liquid-phase 1-propanol[18] and for 1-propanol adsorbed on Pd(111);[3] only the salient features are described below.

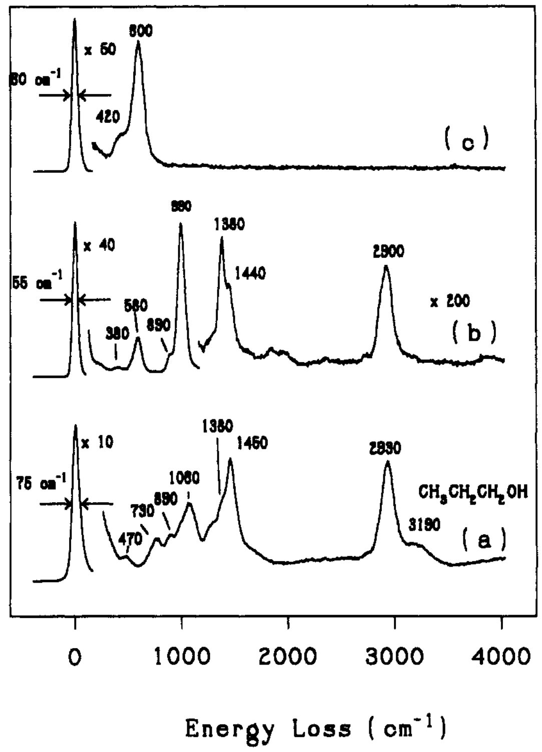

Figure 3. High resolution electron energy loss spectra for (a) condensed 1-propanol at 120 K, (b) condensed 1-propanol annealed to 250 K; and (c) condensed 1-propanol annealed to 800 K.

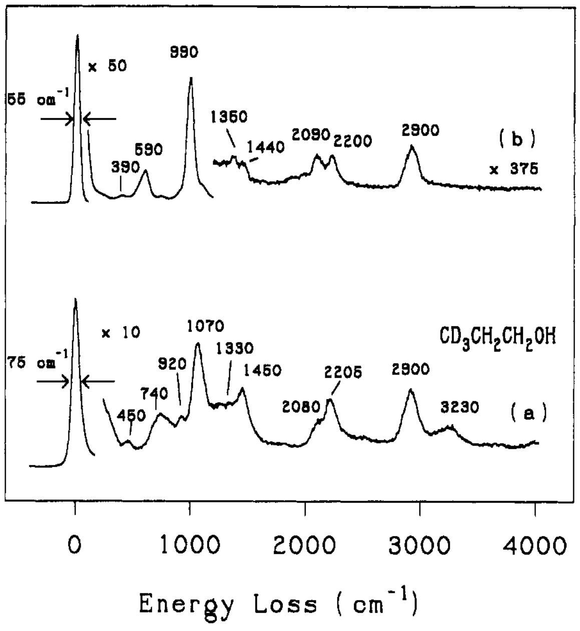

Figure 4. High resolution electron energy loss spectra for (a) condensed 1-propanol-3,3,3-d_3 at 120 K and (b) condensed 1-propanol-3,3,3-d_3 annealed to 250 K.

The losses at ~1380 and 1450 cm^{-1} in the electron energy loss spectra of 1-propoxide, assigned as the $\delta_s(CH_3)$ and $\delta_a(CH_3)$ modes, have different relative intensities compared to condensed 1-propanol (Figures 3a,b and 4a,b). We attribute the intensity redistribution to a preferred orientation in 1-propoxide as compared to a more random orientation distribution for condensed 1-propanol. Off-specular measurements show that these modes arise mainly from dipole scattering.

The losses at ~1380 and 1450 cm^{-1}, Figures 3a and 4a, also contain contributions from the methylene wags and bends as is evident from the residual intensity in this region in the spectrum of 1-propoxide-3,3,3-d_3 for which the $\delta(CD_3)$ modes are shifted to 1090 cm^{-1} (Figure 4a). The methylene bend and wag modes have been observed at these frequencies for gas-phase 1-propanol.[18] The contributions of the wag and bend modes to the intensities of the peaks at 1380 and 1450 cm^{-1} are minor, however, as is clearly evident from comparison of their intensities in Figure 4b to the total intensity in this region from the deformations, bends, and wags in 1-propanol-d_0 (Figure 3b). The weak features in the spectrum of 1-propoxide-3,3,3-d_3 at 1440 and 1350 cm^{-1} are assigned as the CH_2 bend and wag, respectively.[18] Upon deuteration, these modes are shifted down to ~1000 cm^{-1},[19] but, due to their weak intensity, they are not resolved. The demonstrated weak intensity of the CH_2 bending and wagging modes allows us to assign most of the intensity at 1380 and 1440 cm^{-1} to the methyl deformation modes.

The loss in the range of 1050–1070 cm^{-1}, observed for condensed layers of all isotopomers except for 1-propanol-1,1-d_2, is assigned as a combination of the ν(C–C), ν(C–O), and $\rho(CH_3)$ modes (Figures 3 and 4a).[20] These assignments are in agreement with those observed for 1-propanol on Al_2O_3.[21] The assignment of the ν(C–O) mode in this region is preferred rather than an assignment at ~971 cm^{-1}.[18] Assigning the peak at ~1060 cm^{-1} is consistent with the assignment of C–O stretches in alcohols made elsewhere[22] and compares better with what has been observed for other alcohols on Mo(110).[4,23]

The intense loss in the 1-propoxide isotopomer spectra at 975–990 cm^{-1} is assigned as the ν(C–O) mode (Figures 3b and 4b). This loss also contains contributions from other losses including the $\rho(CH_3)$ and $\rho(CH_2)$ modes in the various isotopomer spectra. However, the strong intensity combined with the downshift make the assignment unequivocal. Consistent with the assignment, off-specular data demonstrate that this loss is strongly dipolar in nature; i.e. the loss is strongly peaked close to the specular direction. The strong intensity and high dipolar nature has been seen previously for the ν(C–O) mode in alkoxides on Mo(110).[4,23]

The new loss observed upon formation of the 1-propoxide intermediate in the region of 580–590 cm^{-1} is assigned as the ν(metal–OR) mode. This is in good agreement with values reported for methoxide and 2-propoxide on Mo(110).[4,23] As for 2-propoxide this loss is strongly dipolar in nature, as determined by off-specular experiments.

Some weak losses are observed in the region between 1500 and 2700 cm^{-1} in the spectra of 1-propanol isotopomers. In the spectrum for 1-propoxide-d_0, the loss at ~1980 cm^{-1} is assigned as a double loss of the very intense ν(C–O) mode (Figure 3b). The other weak features at ~1600 and ~1820 cm^{-1} are tentatively assigned as a combination of the ν(C–O) mode stretch with other ν(metal–OR) and ν_s(C–C) modes (Figure 3b). Similar assignments can be made for the other isotopomers.

The ν(C–O) mode is still present in an electron energy loss spectrum of 1-propanol annealed to 400 K along with the other modes observed at 300 K. A new loss at 600 cm^{-1} is assigned as a ν(metal–O) stretch.[4,23] Its intensity increases as a function of temperature, in accord with temperature programmed reaction data in which hydrocarbons and nonselective decomposition products are formed beginning at about 350 K; both reactions deposit oxygen on the surface.

Electron energy loss, Auger electron, and X-ray photoelectron spectroscopies show that atomic carbon and atomic oxygen are left on the surface after reaction to 750 K. No losses are seen that can be attributed to C–C, C–O, or C–H modes in high resolution electron energy loss spectra. The losses seen at 420 and 600 cm^{-1}, Figure 3c, are assigned to a combination of ν(metal–C) and ν(metal–O) modes.

Discussion

We propose that propene elimination and nonselective dehydrogenation arise from competition between C–O bond breaking and dehydrogenation at the 1-carbon in 1-propoxide (Figure 5). High resolution electron energy loss and X-ray photoelectron data clearly indicate that the O–H bond is broken upon adsorption at 120 K and that 1-propoxide is the major intermediate present on the surface when hydrocarbon formation commences. At reaction saturation (0.35 monolayer), ~60% of the 1-propoxide intermediates proceed on to hydrocarbon formation, while the remaining 40% undergo nonselective decomposition to atomic carbon, oxygen, and gaseous H_2. Temperature programmed reaction of isotopically-labeled 1-propanol demonstrates that dehydrogenation at the 1-carbon commences near 350 K, the same temperature regime necessary for propene elimination.

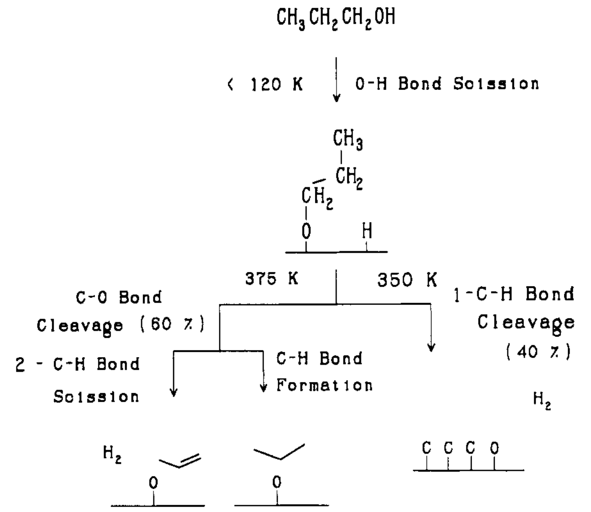

Figure 5. Proposed reaction scheme for the reaction of 1-propanol on Mo(110) at saturation exposure.

Besides aiding in the identification of the 1-propoxide intermediate, the high resolution electron energy loss data provide evidence that the C–O bond is oriented near the surface normal (Figure 5). The relative intensities of the $\delta_a(CH_3)$ and $\delta_s(CH_3)$ modes are used to estimate the orientation of the methyl group.[24,25] Importantly, off-specular measurements establish that dipole scattering predominates for both of these modes, so that the dipole selection rule can be applied and the contributions of the CH_2 wag and bend are minor. The $\delta_s(CH_3)$ dynamic dipole moment is oriented along the C–C axis, while the $\delta_a(CH_3)$ dynamic dipole moment is oriented perpendicular to it. Hence, the dipole contribution to the intensity of the symmetric mode should dominate for nearly perpendicular orientations of the methyl group with respect to the surface, whereas the asymmetric mode should be more intense for orientations more nearly parallel to the surface. Experimentally, the $\delta_s(CH_3)$ mode is considerably more intense than the $\delta_a(CH_3)$ mode, indicating that the methyl group is oriented nearly normal to the surface.[25,26] Hence, the C–O bond is inferred to be nearly perpendicular to the surface, assuming that the carbon centers retain sp^3 hybridization and tetrahedral bond angles. This assumption is warranted based on the correspondence in assignments for 1-propoxide and 1-propanol (Table II). A similar analysis for 2-propoxide likewise indicated a perpendicular C–O bond orientation.[24] A more in-depth study will be published separately.[24].

With the knowledge that 1-propoxide is the major surface intermediate, isotopic labeling methods clearly establish key features of the reaction mechanism; in particular, selective 2-C–H bond breaking is shown to lead to propene formation. A similar selectivity has been observed during propene formation from 2-propoxide.[4] The selectivity for dehydrogenation at the 2-position suggests that C–O bond breaking precedes dehydrogenation in the formation of propene. Facile dehydrogenation at the 1- *not* the 2-position is expected when there is an intact C–O bond since the presence of the electronegative oxygen atom lowers the homolytic C–H bond strength at the 1-carbon. Indeed, selective 1-dehydrogenation is observed for alkoxide reactions in which the C–O bond is retained, such as acetone formation from 2-propoxide on Rh(111)–p(2×1)–O[27] or acetaldehyde formation from ethanol on Cu(110).[5] If the C–O bond is broken prior to dehydrogenation, the preference for dehydrogenation at the 1-carbon is removed and dehydrogenation at the 2-position is anticipated. The lack of a significant kinetic isotope effect in the rate of propene formation upon deuteration of the 2-carbon substantiates the assertion that C–O bond breaking limits the rate of propene formation and that dehydrogenation at the 2-carbon rapidly follows.

Although the 1-C–H bonds are *not* cleaved along the path for propene formation, facile 1-C–H bond cleavage does occur during nonselective decomposition. Indeed, the enhanced selectivity for propene formation from 1-propanol-1,1-d_2 indicates that the rate of 1-C–H bond scission controls the rate of nonselective reaction. Since propene is formed exclusively via 2-C–H bond breaking, 1-C–H(D) bond scission must result in nonselective decomposition. The selectivity for dehydrogenation at the 1-position suggests that it precedes C–O bond breaking and that it is the rate-limiting step for nonselective reaction. Accordingly, the relative rates of dehydrogenation at the 1-carbon and C–O bond breaking will dictate the selectivity for nonselective decomposition versus propene elimination. The rate of 1-C–D bond cleavage in 1-propanol-1,1-d_2 will be slower than for the 1-propanol-d_0, for example, while the rate of C–O bond cleavage is the same. Therefore, the yield of propene should be greater for 1-propanol-1,1-d_2 than for 1-propanol-2,2-d_2, -3,3,3-d_3, or -d_0, as is observed experimentally (Figure 1 inset).

High resolution electron energy loss data also provide evidence that the C–O bond in 1-propoxide is weakened due to the interaction with Mo(110). The loss at 990 cm^{-1} in the electron energy loss spectra of 1-propoxide is assigned as the ν(C–O) mode. This corresponds to a downshift in energy of ~75 cm^{-1} from the gas-phase value of 1064 cm^{-1}. Previously, C–O bond weakening in 2-propoxide was suggested based on the C–O stretching frequency of ~890 cm^{-1} compared to a value of 1072 cm^{-1} in 2-propanol. The frequencies quoted are for saturation coverages, which are the same for the two isomers within experimental error. The frequency of this mode suggests that there is less C–O bond weakening for 1-propoxide compared to 2-propoxide on Mo(110).[28] The origin of this difference is not known and requires theoretical studies.

The relative values of the C–O stretch in 1- and 2-propoxide are consistent with their relative reactivities. Propene elimination occurs more rapidly during the reaction of 2-propoxide than 1-propoxide. On the basis of these data and the assumption that the C–O stretch frequency is related to the bond strength, the C–O bond in 1-propoxide adsorbed on Mo(110) is stronger than its geometric isomer, 2-propoxide. Weakening of the C–O bond is expected to facilitate hydrocarbon formation; therefore, C–O bond breaking is expected to occur more readily in 2-propoxide than for 1-propoxide, as is experimentally observed. Due to coupling of ν(C–O) to other modes in both 1- and 2-propoxide, a more detailed analysis is not possible. Theoretical studies are necessary to probe for the degree of C–O bond weakening upon adsorption for the two cases.

The relative kinetics of propene formation from 2-propoxide and 1-propoxide do not correlate with the strength of the C–H bonds that are broken during propene formation. The C–H bond in the methyl group of 2-propoxide, a primary carbon, is expected to be harder to cleave than the C–H bond in the methylene group of 1-propoxide, a secondary carbon;[29] hence slower kinetics for propene formation from 2-propoxide would be predicted based on C–H bond strength in contrast to experimental results.

In addition to the difference in the initial rate of propene formation observed for reaction of the propoxide isomers, propene is formed from 1-propoxide over a much wider temperature range and with lower selectivity than for 2-propoxide. Propene is formed over a range of ~150 K for 1-propoxide (Figure 1) compared to 80 K for 2-propoxide and the selectivities for propene elimination are 60 and 70% respectively for the 1- and 2-isomers. The broad range of reaction rates for 1-propoxide may arise from the deposition of significant amounts of surface oxygen and hydrocarbon fragments during nonselective decomposition. During the reaction of 2-propoxide, nonselective decomposition does not commence until propene formation has reached a maximum rate. This is probably due to the more rapid kinetics for 2-propoxide deoxygenation and accounts for the higher selectivity. In contrast, C–O bond cleavage is intrinsically slower in 1-propoxide so that nonselective decomposition occurs in the same temperature range as propene formation. Oxygen is deposited during both nonselective reaction and propene elimination, and surface oxygen has been shown previously to stabilize adsorbed alkoxides on Mo(110) with respect to nonselective decomposition.[16,30] The presence of hydrocarbon fragments may also alter reaction kinetics, such as propene formation, although this has not been explicitly investigated.

The proposed rate-limiting C–O bond cleavage in the deoxygenation of alkoxides on Mo(110) is analogous to the desulfurization of thiolates on Mo(110). The relative kinetics for hydrocarbon production during thiolate reaction suggest that C–S bond breaking controls the rate of desulfurization. For example, the tertiary thiol, *tert*-butyl thiolate forms isobutene and isobutane via C–S bond cleavage at lower temperature than hydrocarbon formation from reaction of primary thiols.[31]

The specific comparison of 1-propanol and 1-propanethiol, its sulfur-containing analogue, substantiates the argument that C–O and C–S bond breaking control their respective rates of reaction. 1-Propanethiol produces 1-propyl thiolate upon adsorption at 120 K on Mo(110).[32,33] The same gaseous products, dihydrogen, propene, and propane, are produced from both 1-propoxide and 1-propyl thiolate.[33] However, the temperatures required for C–S bond cleavage are substantially lower than for C–O bond cleavage. 1-Propyl thiolate undergoes C–S bond cleavage to form gaseous products at ~250 K, ~100 K lower than that required to cleave C–O bonds in 1-propoxide. Since a C–O bond is ~20 kcal/mol stronger than a C–S bond, the faster kinetics for the thiolate decomposition are consistent with the relative strengths of C–S and C–O bonds. Hence, the selectivity is higher for propane formation in the reaction of 1-propyl thiolate than that in 1-propanol.

In addition to the relative strengths of the C–S and C–O bonds, a decreased mobility of adsorbed hydrogen on the surface may play a role in decreasing the rate of hydrogen addition to 1-propoxide. We have observed that the kinetics for hydrogen atom recombination are altered by the presence of oxygen-containing intermediates, including 1-propoxide, suggesting that the interaction of hydrogen with the surface is altered. Dihydrogen recombination occurs at 425 K during the reaction of 1- and 2-propanol on Mo(110), compared to 350 K on a clean Mo(110) surface. On the other hand, dihydrogen recombination commences at 300 K during the reaction of 1-propyl thiolate, 50 K lower than recombination of dihydrogen on Mo(110).[34] Although the origin of this difference is unknown, the same effects at work in decreasing the rate of hydrogen atom recombination may play a role in hydrogen addition to the 1-propoxide intermediate.

Conclusions

1-Propanol reacts via three competing pathways on Mo(110): deoxygenation and dehydrogenation to form propene (major product), C–O bond hydrogenolysis to form propane, and nonselective decomposition to gaseous dihydrogen, surface carbon, and surface oxygen. The reaction of isotopically-labeled 1-propanols shows that dehydrogenation only occurs at the 2-carbon during propene formation. Secondly, 1-C–H bond scission, leads to nonselective decomposition at 375 K. Electron energy loss data indicate that the C–O bond is weakened in the 1-propoxide intermediate, however, not as much as previously seen for 2-propanol. In fact, 1-propanol reacts more slowly than either 2-propanol or 1-propanethiol. These differences in reaction kinetics are attributed, in part, to the stronger C–O bond in the 1-propoxide intermediate as compared to the 2-propoxide and 1-propyl thiolate intermediates, with C–O bond scission being the rate-limiting step. Orientational analysis using electron energy loss data provides evidence for the C–O bond vector being nearly normal to the surface.

Acknowledgment. This work was supported by the Department of Energy, Basic Energy Sciences, Grant No. DE-FG02-84ER13289. P.C.U. thanks and acknowledges Harvard University for support of a Postdoctoral Fellowship.

Registry No. 1-Propanol, 71-23-8; molybdenum, 7439-98-7; 1-propoxide, 16499-18-6.

J. Phys. Chem. **1992**, *96*, 5069–5077 **5069**

Supplementary Material Available: Tables of vibrational assignments for 1-propanol-1,1-d_2, -2,2-d_2, and -3,3,3-d_3 and figures showing HREEL spectra for 1-propanol-1,1-d_2 and -2,2-d_2 (5 pages). Ordering information is given on any current masthead page.

References and Notes

(1) Benziger, J. B.; Madix, R. J. *J. Catal.* **1980**, *65*, 36.
(2) Davis, J. L.; Barteau, M. A. *Surf. Sci.* **1987**, *187*, 387.
(3) Davis, J. L.; Barteau, M. A. *Surf. Sci.* **1990**, *235*, 235.
(4) Uvdal, P.; Wiegand, B. C.; Friend, C. M. Submitted for publication in *J. Chem. Phys.*
(5) Bowker, M.; Madix, R. J. *Surf. Sci.* **1982**, *116*, 549.
(6) Brainard, R. L.; Madix, R. J. *Surf. Sci.* **1989**, *214*, 396.
(7) Brainard, R. L.; Madix, R. J. *J. Am. Chem. Soc.* **1989**, *111*, 3826.
(8) Wang, J.; Masel, R. I. *J. Catal.* **1990**, *126*, 519.
(9) Wiegand, B. C.; Friend, C. M.; Roberts, J. T. *Langmuir* **1989**, *5*, 1292.
(10) Roberts. J. T.; Friend, C. M. *J. Am. Chem. Soc.* **1986**, *108*, 7204.
(11) This ratio was calculated by measuring the temperature programmed reaction peak areas for m/e 41 and 43. The m/e 43 area was corrected for ^{13}C natural abundance in propene. Then $^1/_2$ the area of the m/e 43 peak was subtracted from the m/e 41 area, since propane fragments to m/e 41. Finally, the m/e 43 area was multiplied by 2.5 to account for the fact that m/e 43 is only 13% of the total propane fragments, while m/e 41 amu is 32% of the propene fragments.
(12) The fragmentation pattern of the propane-d_2 was estimated by using propane-d_0 as a reference.
(13) The relative yields of propene from the 1-propanol isotopomers were based on integration of the area in the spectra of the partent ion of each of the isotopomers. Small differences in the fragmentation patterns of the various isotopomers would introduce only insignificant errors into this approximation. For propene-d_2 and propene-d_3, these were measured and were determined not to be a problem. Similar experiments were unable to be performed on propene-d_1, since we did not have the chemical.
(14) Gelius, U.; Heden, P. F.; Hedman, J.; et al. *Phys. Scr.* **1970**, *2*, 70.
(15) Liu, A. C.; Friend, C. M. *J. Chem. Phys.* **1988**, *89*, 4396.
(16) Liu, A. C.; Friend, C. M. *Surf. Sci.* **1989**, *216*, 33.
(17) Our previous coverage calibration was in error. The oxygen overlayer previously thought to have a coverage of 0.33 monolayer actually has a coverage of 0.45, which is used as a reference state in this work.
(18) Fukushima, K.; Zwolinski, B. J. *J. Mol. Spectrosc.* **1968**, *26*, 368.
(19) McMurry, H. L.; Thornton, V. *J. Chem. Phys.* **1951**, *19*, 1014.
(20) This region has been assigned in terms of the multiple modes observed in the infrared spectra of gas-phase 1-propanol and its deuterated analogues.[35]
(21) Williams, S. D.; Hipps, K. W. *J. Catal.* **1982**, *78*, 96.
(22) *Spectrometric Identification of Organic Compounds*, 4th ed.; Silverstein, R. M., Bassler G. C., Morrill, T. C., Eds.; John Wiley and Sons: New York, 1981.
(23) Wiegand, B. C.; Uvdal, P.; Friend, C. M. Manuscript in preparation.
(24) Uvdal, P.; Wiegand, B. C.; Friend, C. M. Manuscript in preparation.
(25) Bent, B. E.; Mate, C. M.; Crowell, J. E.; Koel, B. E.; Somorjai, G. A. *J. Phys. Chem.* **1987**, *91*, 1493.
(26) Data for selectively-labeled 1-propoxide was key to making the orientational determination. Importantly, electron energy loss spectra of 1-propoxide and 1-propoxide-3,3,3-d_3 show that the losses around 1400 cm^{-1} in the propoxide spectra are mainly due to the $\delta(CH_3)$ modes (Figures 3b and 4b; Tables II and III).
(27) Xu, X.; Friend, C. M. *Surf. Sci.* **1992**, *260*, 15.
(28) The shift in the ν(C–O) mode to lower frequency upon formation of the alkoxide for the different alcohols is proposed to be due to weakening of C–O bond. A simple mass effect as a result of changing the bonding of oxygen from a hydrogen to a molybdenum is excluded, since similar shifts would be expected to be observed for both 1-propoxide (990 cm^{-1}) and 2-propoxide (890 cm^{-1}). The large difference in the shifts for the two alkoxides contradicts the simple mass effect.
(29) Kerr, J. A. *Chem. Rev.* **1966**, *66*, 465.
(30) Serafin, J. G.; Friend, C. M. *J. Am. Chem. Soc.* **1989**, *111*, 8967.
(31) Wiegand, B. C.; Uvdal, P.; Friend, C. M. Submitted for publication in *J. Phys. Chem.*
(32) Roberts, J. T.; Friend, C. M. *J. Am. Chem. Soc.* **1987**, *109*, 3872.
(33) Roberts, J. T.; Friend, C. M. *Surf. Sci.* **1988**, *198*, L321.
(34) Roberts, J. T.; Friend, C. M. *Surf. Sci.* **1987**, *186*, 201.
(35) Wiegand, B. C.; Uvdal, P. Unpublished results.
(36) The β_1 peak includes integration of the area in the hydrogen isotope peak at temperatures up to 475 K, while the β_2 area was above 475 K.
(37) The modes in the 700–900-cm^{-1} region could not be assigned in detail for condensed 1-propanol and its deuterated analogues due to lack of resolution. However, $\rho(CH_3)$, $\gamma(CH_2)$, ν(C–C), and $\rho(CH_2)$ modes have been observed in this energy region for gaseous 1-propanol,[18] 1-propoxide,[3] and both nondeuterated and deuterated gaseous propane.[19]
(38) The loss at 1130 cm^{-1} for condensed 1-propanol-1,1-d_2 and the loss at 1195 cm^{-1} for 1-propanol-2,2-d_2 are proposed to be related to deuteration of the methylene group. Modes in this energy region have been observed previously for propane-2,2-d_2[19] and were associated with coupling of $\rho(CH_3)$ and ν(C–C) modes (1130 cm^{-1}), as well a CD_2 wag mode (1199 cm^{-1}). However, an unequivocal assignment of the observed losses could not be made.

In Situ Fourier Transform Infrared Study of Ethylene Surface Reaction Kinetics on Alumina-Supported Nickel

Mark P. Lapinski[†] **and John G. Ekerdt***

Department of Chemical Engineering, University of Texas at Austin, Austin, Texas 78712

(Received: January 10, 1992)

A method for obtaining kinetic parameters for hydrocarbon surface reactions with FTIR is described and demonstrated for two C_2 surface species. The surface species resulted from initial doses of either C_2H_4 or C_2D_4 on Ni/Al_2O_3, which was precovered with H(D), at 195–240 K. Kinetic parameters were obtained by observing characteristic infrared band intensities of the adsorbed species as a function of time at constant temperature. The decomposition of $\sigma\pi$-ethylene and the formation of ethylidyne were well modeled by a second-order expression of the form rate = KC_A^2. A H–D isotope effect was observed for both the surface reactions signifying the importance of C–H(D) scission and formation reactions in the rate-limiting step. The activation energies for the decomposition of $\sigma\pi$-C_2H_4 and $\sigma\pi$-C_2D_4 on Ni/Al_2O_3 were found to be 7.9 and 10.2 kcal/mol, respectively. For the formation of CCH_3 and CCD_3 on Ni/Al_2O_3, activation energies of 5.1–8.7 and 4.3–6.4 kcal/mol were found, respectively. Preadsorbed hydrogen, high ethylene doses, and ethylene–metal bond strengths may have contributed to the second-order formation of ethylidyne on Ni/Al_2O_3.

Introduction

Numerous studies of small, unsaturated molecules, such as ethylene and acetylene, have been conducted over transition-metal surfaces to identify the adsorbed structures and to characterize the changes in adsorbed species with changes in temperature. These studies can help understand the factors that influence activity and selectivity and serve as a model for understanding larger hydrocarbon molecules that contain unsaturated bonds. By measurement of the rates of surface transformations, kinetic parameters can be determined. Comparisons can then be made to the kinetic parameters of related catalytic reactions and to theoretical predictions.

One of the most studied surface reactions is the formation of ethylidyne (CCH_3) from the adsorption of ethylene. Many different techniques have been used to determine the kinetic parameters. For example, on Pt(111), the ethylidyne formation

---

[†] Present address: Exxon Research and Development Laboratories P.O. Box 2226, Baton Rouge, LA 70821.
* To whom correspondence should be addressed.

0022-3654/92/2096-5069$03.00/0